Nephrol Dial Transplant (2018) 33: 1333–1343
doi: 10.1093/ndt/gfx354
Advance Access publication 19 January 2018

ORIGINAL ARTICLE

Role of the cytochrome P-450/ epoxyeicosatrienoic acids pathway in the pathogenesis of renal dysfunction in cirrhosis

Michael M. Yeboah[1], Md. Abdul Hye Khan[2], Marla A. Chesnik[1], Melissa Skibba[2], Lauren L. Kolb[2] and John D. Imig[2]

[1]Department of Medicine, Medical College of Wisconsin, Milwaukee, WI, USA and [2]Department of Pharmacology and Toxicology, Medical College of Wisconsin, Milwaukee, WI, USA

Correspondence and offprint requests to: Michael M. Yeboah; E-mail: mmyeboah@mcw.edu

ABSTRACT

Background. Hepatorenal syndrome (HRS) is a life-threatening complication of advanced liver cirrhosis that is characterized by hemodynamic alterations in the kidney and other vascular beds. Cytochrome P(CYP)-450 enzymes metabolize arachidonic acid to epoxyeicosatrienoic acids (EETs) and 20-hydroxyeicosatetraenoic acids. These eicosanoids regulate blood pressure, vascular tone and renal tubular sodium transport under both physiological and pathophysiological states.

Methods. Experiments were performed to investigate the role of the CYP system in the pathogenesis of renal dysfunction during cirrhosis. Rats underwent bile duct ligation (BDL) or sham surgery and were studied at 2, 4 and 5 weeks post-surgery. In additional experiments, post-BDL rats were treated with three daily intraperitoneal doses of either the selective epoxygenase inhibitor *N*-(methylsulfonyl)-2-(2-propynyloxy)-benzenehexanamide (MSPPOH) or a vehicle, starting on Day 22 after surgery.

Results. BDL led to progressive renal dysfunction that was associated with reduced renal cortical perfusion but without any overt histologic changes, consistent with HRS. CYP isoform enzyme expression was significantly altered in BDL rats. In the kidney, CYP2C23 expression was upregulated at both the mRNA and protein levels in BDL rats, while CYP2C11 was downregulated. Histologically, the changes in CYP2C23 and CYP2C11 expression were localized to the renal tubules. EET production was increased in the kidneys of BDL rats as assessed by urinary eicosanoid levels. Finally, treatment with the selective epoxygenase inhibitor MSPPOH significantly reduced renal function and renal cortical perfusion in BDL rats, suggesting a homeostatic role for epoxygenase-derived eicosanoids.

Conclusions. The CYP/EET pathway might represent a novel therapeutic target for modulating renal dysfunction in advanced cirrhosis.

Keywords: cirrhosis, cytochrome P-450, epoxyeicosatrienoic acids, hepatorenal syndrome

INTRODUCTION

Hepatorenal syndrome (HRS) is a common and severe complication of advanced cirrhosis and fulminant acute liver failure. It occurs in 11% of cirrhotics with refractory ascites and is associated with very high mortality [1–6]. HRS is the result of profound hemodynamic derangement that is initiated by portal hypertension and is characterized by intense intrarenal vasoconstriction in the setting of marked visceral vasodilatation [4, 7, 8]. Portal hypertension leads to increased shear stress in the splanchnic vasculature, which in addition to bacterial translocation from the bowel and the associated systemic inflammatory response, results in the generation of endogenous vasodilators like nitric oxide (NO) and prostacyclins that are responsible for splanchnic vasodilatation, pooling of blood and reduced effective circulating blood volume [9–13]. The foregoing initially leads to the establishment of a hyperdynamic circulation that involves increased heart rate and cardiac output [14, 15]. As the liver cirrhosis advances, neurohumoral vasoconstrictor mediators like the sympathetic nervous system (SNS), renin–angiotension–aldosterone system (RAAS) and vasopressin are activated. These vasoconstrictor mechanisms, while necessary for maintaining an adequate circulating blood volume, are associated with detrimental vasoconstriction in many organs. In the kidney, the consequences include afferent arteriolar vasoconstriction, reduction in blood flow, decreased glomerular filtration rate (GFR) and salt and water retention that causes ascites and volume overload [16–19].

Despite the significant advances in our understanding of the pathophysiology and treatment of this potentially fatal condition in the past two decades, the knowledge is incomplete and this has limited therapeutic options for patients with HRS. Importantly, the effectiveness of the current pharmacological therapies is only modest and they are mostly used as a bridge to liver transplantation [20–22]. Therefore, novel treatment options are needed to improve the long-term survival of these patients.

Arachidonic acid (AA) is metabolized by key enzymes to small molecule mediators with diverse pathophysiological effects [23]. Specifically, the cytochrome P (CYP)-450 enzymes have two main pathways: epoxygenases (mostly the CYP2C and CYP2J family of enzymes) metabolize AA to four bioactive regioisomeric epoxyeicosatrienoic acids (EETs; 5,6-EET, 8,9-EET, 11,12-EET and 14,15-EET) and omega-hydroxylases (mostly the CYP4A family of enzymes in the rat) metabolize AA to 20-hydroxyeicosatetraenoic acid (20-HETE). EETs are produced in many tissues, including the kidney, heart, lung and liver, and possess anti-inflammatory and other renoprotective effects. EETs act as endothelium-dependent hyperpolarizing factors (EDHFs) on the renal microcirculation, mediating vasodilatory effects, in addition to regulation of renal tubular water and sodium absorption. On the other hand, 20-HETE constricts afferent arterioles and participates in renal blood flow autoregulation [24–30].

In this study we examined the hypothesis that the CYP/EET system modulates renal dysfunction during cirrhosis.

MATERIALS AND METHODS

Materials

All chemicals were purchased from Sigma-Aldrich (St Louis, MO, USA) unless otherwise noted. Anti-CYP2C23, CYP2C11 and CYP4A1 antibodies were prepared by Dr J. Capdevila (Vanderbilt University, Nashville, TN, USA). *N*-(methylsulfonyl)-2-(2-propynyloxy)-benzenehexanamide (MSPPOH) (CAS 206052-02-0) was purchased from Cayman Chemical (Ann Arbor, MI, USA).

Animals

Male Sprague Dawley rats weighing 225–250 g (Envigo, Indianapolis, IN, USA) were used. Animals were kept in a temperature-controlled environment with a 12-h light–dark cycle and were allowed free access to water and standard rat chow. Rats were acclimatized for a minimum of 1 week before experimentation. All animals received humane care in compliance with the National Research Council's Guide for the Care and Use of Laboratory Animals. The animal protocol was approved by the Institutional Animal Care and Use Committee of the Medical College of Wisconsin.

Animal model of liver cirrhosis

Liver cirrhosis was induced in rats by common bile duct ligation (BDL) [31–33]. Laparotomy was performed under anesthesia with isoflurane. The bile duct was isolated, doubly ligated with 4-0 silk and resected between the two ligatures. The abdominal wall was closed with 4-0 Vicryl sutures and the skin was closed with 9-mm wound clips. Sham operation was performed similarly, but without ligation and resection of the bile duct. Some animals that had already undergone BDL surgery were also obtained from the vendor. Animals were studied 2, 4 and 5 weeks after surgery. The rats were individually placed in metabolic cages for 24-h urine collection prior to euthanasia and blood collection. Liver injury was evaluated by measuring serum levels of total bilirubin (Marshfield Labs, Waukesha, WI, USA).

MSPPOH-treated animals

Beginning on Day 22 after BDL surgery, animals received daily intraperitoneal injections of a vehicle or the selective epoxygenase inhibitor MSPPOH (20 mg/kg) for 3 days. The administered dose was chosen on the basis of the drug's pharmacokinetic properties and is similar to the dose used in recent *in vivo* experiments [34].

Assessment of renal perfusion

Animals were anesthetized with 60 mg/kg pentobarbital administered intraperitoneally. Laparotomy was performed to expose the left kidney. Renal blood flow was measured via laser Doppler flowmetry with Perimed PF5010 LDPM unit (PeriFlux System 500, Stockholm, Sweden). A Doppler flow probe was carefully placed on the surface of the kidney to measure cortical blood flow. The mean cortical blood flow was calculated from three consecutive measurements recorded at 5-min intervals after stabilization.

Biochemical analysis

Blood urea nitrogen (BUN) was measured spectrophotometrically using a commercial kit (BioAssay Systems, Hayward, CA, USA). Serum and urine creatinine levels were measured by isotope dilution liquid chromatography (LC)–dual mass spectrometry (MS/MS) (University of Alabama at Birmingham–University of California at San Diego O'Brien Core Center for Acute Kidney Injury Research). Urine and serum sodium were measured using a Dual-Channel Flame Photometer 02655-10 (Cole-Parmer, Vernon Hills, IL, USA). Urine protein was measured by detergent compatible protein assay (BioRad, Hercules, CA, USA). Urinary *N*-acetyl-β-D-glucosaminidase (NAG) activity was measured with a commercial kit (Crystal Chem, Downers Grove, IL, USA) according to the manufacturer's instructions.

Measurement of urine EET levels

Urinary CYP metabolite levels were measured by LC-electrospray ionization (ESI)-MS/MS. Samples were prepared from 200 μL of urine from individual rats using solid-phase extraction with a Varian Bond Elut C18 Column (Agilent Technologies, Santa Clara, CA, USA). Deuterated internal standards (ISs) for each class of lipid component were added before extraction: 1.6 ng each of d_{11}-(±)14,15-dihydroxy-5Z,8Z,11Z-eicosatrienoic acid and d_{11}-(±)14,15-epoxy-5Z,8Z,11Z-eicosatrienoic acid for the dihydroxyeicosatrienoic acids (DHETs) and EETs, respectively. The extracted samples were stored at −80°C. Before analysis samples were warmed to 25°C, dried in a stream of nitrogen, reconstituted in 20 μL of acetonitrile and then 12 μL was injected. Components were resolved on a 250 mm × 2.0 mm Kromasil C18 Column packed with 5-μm diameter particles with 100 Å pores. Gradient elution from 80% A to 10% A was used with eluant flow of 0.2 mL/min. Solvent A was water with 0.01% formic acid and solvent B was acetonitrile with 0.01% formic acid using the following

profile: 20% B to 30% B in 10 min, 30% B to 60% B in 17 min, 60% B to 90% B in 28 min, hold at 100% for 7 min, then 7-min re-equilibration. Multiple reaction monitoring (MRM) analysis was performed on an Agilent 6460 triple quadrupole mass spectrometer equipped with a Jet Stream Interface. Precursor ion, product ion, collision energy and fragmenter voltage were optimized for each compound and IS in negative ion mode. Other parameters were as follows: drying gas flow, 10 L/min at 325°C; nebulizer, 20 psi; sheath gas flow, 11 L/min at 325°C; capillary, 3.5 kV; nozzle, 1.0 kV. Results were acquired at unit-mass resolution. The intraday variability is 4–5%. The limit of quantitation for DHETs and EETs was 1 pg/μL at an $S/N > 3$, while the limit of detection was usually <1 pg/μL. Before samples were analyzed, standard curves were run from 1 to 100 pg/μL.

Histological and immunohistochemical analyses

Formalin (10%)-fixed kidney samples were embedded in paraffin. Sections (4 μm) were prepared and used for hematoxylin and eosin and immunohistochemical staining as previously described [30].

Quantitative real-time polymerase chain reaction (PCR)

Quantitative amplification of the cDNA prepared from kidney tissues was performed as previously described [30]. Results were normalized to PGK1 content by the comparative Ct method and relative mRNA levels are expressed as fold change compared with the sham animals. The primer sequences (Integrated DNA Technologies, Coralville, IA, USA) are listed in Table 1.

Western blot analysis

Samples of frozen tissue were homogenized in radioimmunoprecipitation assay buffer containing a protease and phosphatase inhibitor cocktail (Sigma, St Louis, MO, USA). The protein concentration was quantified using the bicinchoninic acid (BCA) Protein Assay (Pierce Biotechnology, Rockford, IL, USA). Proteins (60 μg/lane) were separated by sodium dodecyl sulphate–polyacrylamide gel electrophoresis and transferred to a polyvinylidene fluoride membrane (Bio-Rad, Hercules, CA, USA). After blocking with 5% milk in Tris-buffered saline plus 0.1% Tween-20, the membrane was then incubated with primary antibody (1:1000) for 1 h at room temperature. The blot was then incubated with the appropriate horseradish peroxidase–conjugated secondary antibody (1:5000) for 1 h at room temperature. After washing, protein bands were detected using SuperSignal West Femto Maximum Sensitivity Substrate (Thermo Fisher, Waltham, MA, USA). Blot images were collected on a BioRad Chemidoc System and quantitated via densitometry using ImageQuant TL version 8.1 software. Membranes were stripped and reprobed to allow for the analysis of more than one protein on the same blot.

Statistical analysis

All data are reported as mean±SEM. Statistical significance between two measurements was determined by the two-tailed unpaired Student's *t*-test, using GraphPad Prism version 6.0 software (GraphPad Software La Jolla, CA, USA). P-values ≤ 0.05 were considered statistically significant. The rationale for the number of animals used was based on both review of the literature involving comparable studies and also by power calculation. In order to detect a significant difference in the expression of CYP2C23 between the BDL and sham animals, we selected an α (probability of type I error) of 5% and a β (probability of type 2 error) of 20% (implying a power $1-\beta$ of 80%). With these parameters, we determined the total sample size to be 14 (7 in each group). To further guarantee the statistical power of the study, we increased the total sample size to 16. For experiments involving the administration of epoxygenase inhibitor and using similar parameters as above, we determined the total sample size for the treated and untreated groups to be four (two in each group). To further guarantee the statistical power, we increased the total sample size to seven.

RESULTS

BDL leads to chronological changes in the liver, including an initial phase of surgical jaundice (this phase is reversible), through the development of portal hypertension and biliary fibrosis, then secondary biliary cirrhosis, which is progressive and irreversible and is clinically associated with the development of ascites and jaundice. Previous studies have shown the establishment of portal hypertension as early as 1–2 weeks post-BDL in rats [32]. By 5 weeks, all the BDL animals were jaundiced, had ascites and had an enlarged, nodular and yellow-stained liver surface. The markedly elevated serum bilirubin levels at the 5-week time point confirm the presence of severe liver dysfunction in the BDL rats compared with sham-operated rats (6.3 ± 0.3 versus 0.117 ± 0.017 mg/dL, $P < 0.001$).

BDL is associated with decreased salt excretion by the kidneys

Abnormal renal handling of water and salt is a prominent complication of liver cirrhosis. At the end of 5 weeks post-surgery, urine output was not statistically different between the

Table 1. qPCR primer sequences

Gene	Forward	Reverse
PGK1	CCAAACAATCTGCTTAGCTCG	GATGAGAATGCAAAGACTGGC
CYP2C23	GCAGCTTCATCTTGTCCTTCA	CTCCTGCTCCTTATGAAGTATCC
CYP2C11	ACGTTCTATCTCTTCCTGGACT	GGTGGCTACTGTAACTGACAT
CYP4A1	CCACAATCACCTTCATCTCACT	ACACAGCCACTCATTCCTG
CYP4A2	GAGGATGTCATAGTGGAAGGC	AGATCCAAAGCCTTATCAATCCC
CYP4A3	TCTCGACTCACAGAAGGTACT	CACCAAGAGAGATGCAGAGAG
CYP4A8	TCCTGTCCAACAATCTGTTCC	ACTCCAGCTTTCCACTATGAC

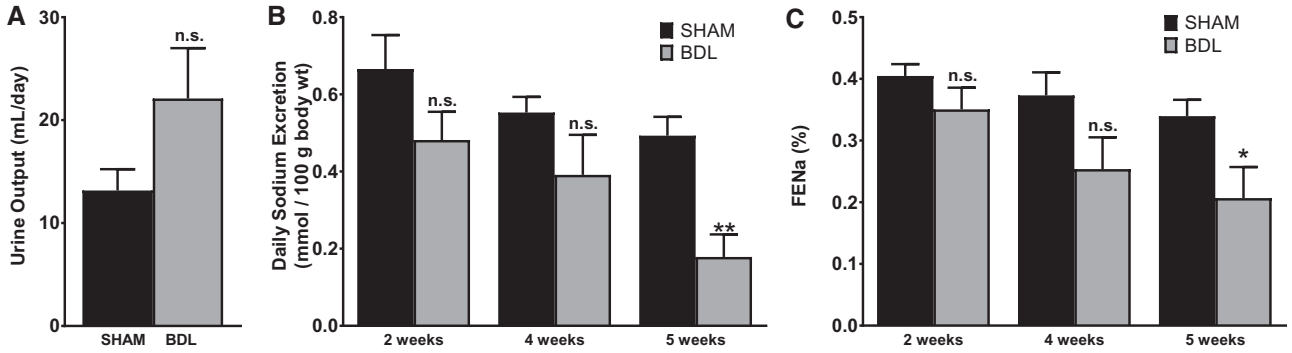

FIGURE 1: BDL is associated with decreased salt excretion by the kidneys.
A rat model of cirrhosis was established by BDL. The animals were placed individually in metabolic cages and a 24-h urine sample was collected before blood collection. Blood and urinary sodium was measured as described in the 'Materials and Methods' section and fractional excretion of sodium (FE_{Na}) was calculated. (**A**) Total urine output at 5 weeks after BDL or sham surgery. (**B**) Sodium excretion rate at various time points. (**C**) FE_{Na} at various time points. Values are represented as the mean ± SEM; $n = 7–10$ per group. *$P < 0.05$, **$P < 0.001$ versus sham group.

BDL and sham-operated animals (Figure 1A). A trend toward decreased daily sodium excretion rate developed as early as 2 weeks in BDL animals, persisted at 4 weeks and was significantly reduced at 5 weeks compared with sham animals (Figure 1B). Importantly, fractional excretion of sodium trended down in a time-dependent manner and was significantly reduced in BDL rats at 5 weeks (Figure 1C). This indicates that the observed difference in the sodium excretion rate is due to increased reuptake of sodium by tubular epithelial cells rather than differences in weight or salt intake. These data are in agreement with results of previous studies [32, 33] and show a sodium avid state in this model that is consistent with the development of ascites in the BDL animals.

BDL is associated with functional renal failure in rats

Varying degrees of renal dysfunction occur frequently in patients with cirrhosis. To examine the effect of BDL on renal function, creatinine clearance (CrCl) was measured and used as an index of glomerular filtration rate and renal function. As shown in Figure 2A, CrCl was decreased by ∼34% at both 2 and 4 weeks post-surgery in BDL rats and was reduced by 55% at 5 weeks in BDL rats compared with their sham counterparts. Similarly, at 5 weeks, BUN was 1.9-fold higher in the BDL rats compared with sham rats (Figure 2B). In keeping with the significant decrease in renal function, renal cortical blood flow, as assessed by laser Doppler flowmetry, was markedly reduced in BDL rats compared with sham rats (Figure 2C). Interestingly, despite the significant decrease in renal function in the BDL rats, no overt acute or chronic changes were observed on histological examination of the kidneys. Some tubular epithelial cells in the cortex were stained brown, likely from bilirubin uptake, but there were no features that were typical of acute tubular necrosis (Figure 3A). Consistent with the histological findings and in support of a functional renal impairment in the BDL rats, there was no significant difference in the proteinuria rates in BDL and sham-operated animals at 5 weeks (Figure 3B), suggesting that there are no significant irreversible chronic kidney changes in the BDL rats compared with sham rats. To assess proximal tubular integrity in this model, we measured urinary concentrations of NAG, which is generally accepted as a marker of proximal tubular dysfunction. The level of enzymuria was not significantly different between BDL and sham rats, indicating that the renal dysfunction is mostly hemodynamically mediated (Figure 3C).

Renal CYP enzyme expression is altered during cirrhosis

To investigate the impact of cirrhosis on CYP enzyme abundance in the kidney, we first examined the gene expression patterns of key CYP isoforms in the renal cortex using quantitative PCR (qPCR) at different time points after BDL or sham surgery. As shown in Figure 4, CYP2C23 mRNA was increased by 60, 40 and 90%, respectively, in BDL rats at 2, 4 and 5 weeks compared with sham rats. Conversely, CYP2C11 mRNA levels were reduced by >98% at 2 weeks and were almost non-detectable in the 4- and 5-week samples from BDL rats compared with sham-operated control rats. CYP4A1 mRNA expression was increased by 140, 100 and 240%, respectively, in BDL rats at 2, 4 and 5 weeks compared with sham rats. The expression of other CYP4A isoform genes (CYP4A2, CYP4A3 and CYP4A8) was not significantly different between BDL and sham rats at 5 weeks (data not shown). We also examined CYP protein expression in the renal cortex at 5 weeks post-BDL or sham surgery by western blot analysis. As shown in Figure 5, CYP2C23 protein expression was increased by 47%, whereas CYP2C11 protein expression was reduced by 33% in BDL rats compared with sham rats. CYP4A1 protein expression was reduced by 18% in BDL rats compared with sham rats, but this did not reach statistical significance. The discrepancy between the gene and protein expression data for CYP4A1 is likely because the CYP4A1 antibody recognizes other CYP4A isoform proteins in addition to CYP4A1. Immunohistochemical analysis was conducted to substantiate the western blot findings and also to localize the changes in CYP2C23 and CYP2C11 in kidney sections. At 5 weeks after sham surgery, CYP2C23 immunostaining was predominantly localized in cortical tubules. There was relatively less staining in the medullary tubules. The extent and intensity of CYP2C23 staining increased significantly in BDL rats compared with the sham rats (Figure 6A, B). CYP2C11 was

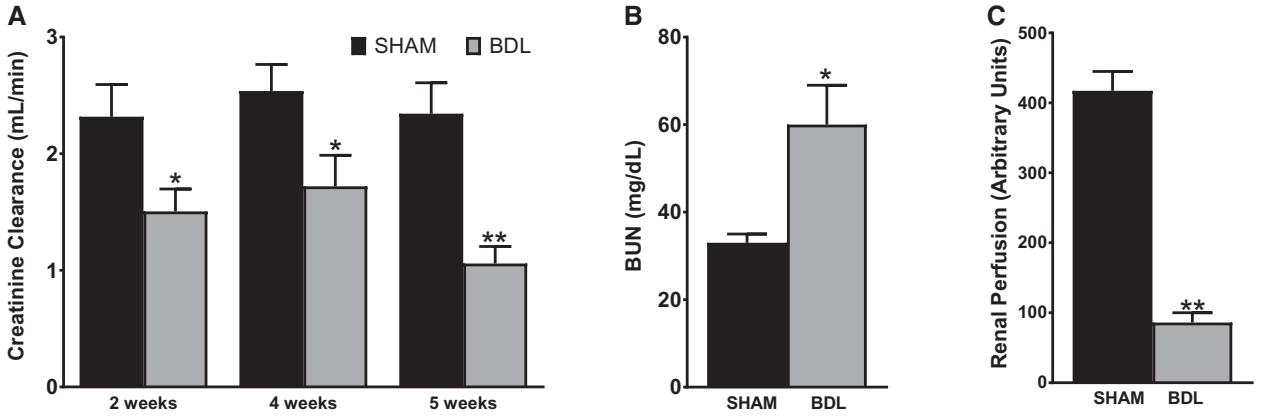

FIGURE 2: BDL is associated with functional renal failure in rats.
A 24-h urine sample was collected from animals placed in metabolic cages followed by blood collection. Urinary and serum creatinine were measured and CrCl was calculated. (**A**) CrCl at various time points, (**B**) BUN and (**C**) renal perfusion pressure were measured in rats 5 weeks after sham or BDL surgery, as described in the 'Materials and Methods' section. Values are represented as the mean ± SEM; $n = 8$ per group. *P < 0.05, **P < 0.001 versus sham group.

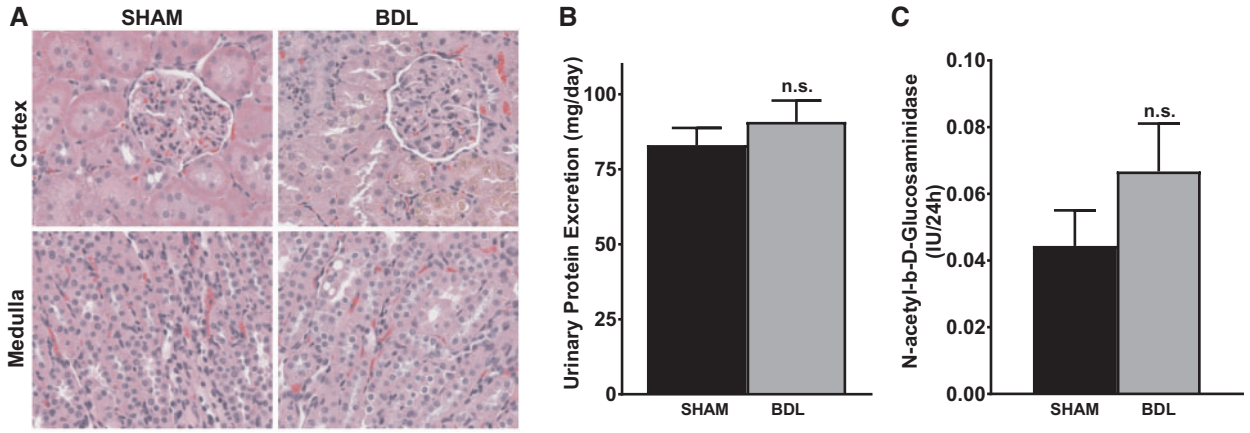

FIGURE 3: Renal dysfunction in BDL rats occurs without major structural damage.
(**A**) Representative hematoxylin and eosin staining of kidney sections from 5-weeks BDL and sham rats. No major acute or chronic changes were observed on histological examination of the kidneys. Original magnification of slides, ×400. (**B**) Protein excretion rate was measured using a 24-h urine sample and was not statistically different between the two groups. (**C**) Urinary NAG level was measured in 4-weeks BDL and sham rats and was not statistically significant (n.s.) between the two groups; $n = 6–8$. Values are represented as the mean ± SEM.

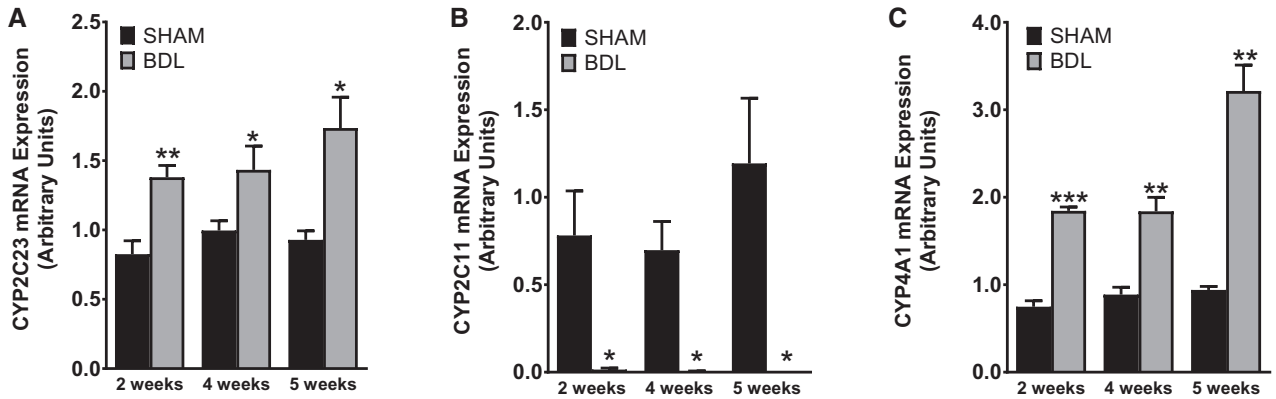

FIGURE 4: BDL leads to altered gene expression of CYP isoforms.
Quantitative real-time PCR was conducted using total mRNA to investigate changes in (**A**) *CYP2C23*, (**B**) *CYP2C11* and (**C**) *CYP4A1* gene expression in renal cortical tissue from rats at various time points after sham or BDL surgery. Values are represented as the mean ± SEM; $n = 7–8$ per group. *P < 0.05, **P < 0.001, ***P < 0.0001 versus the sham group.

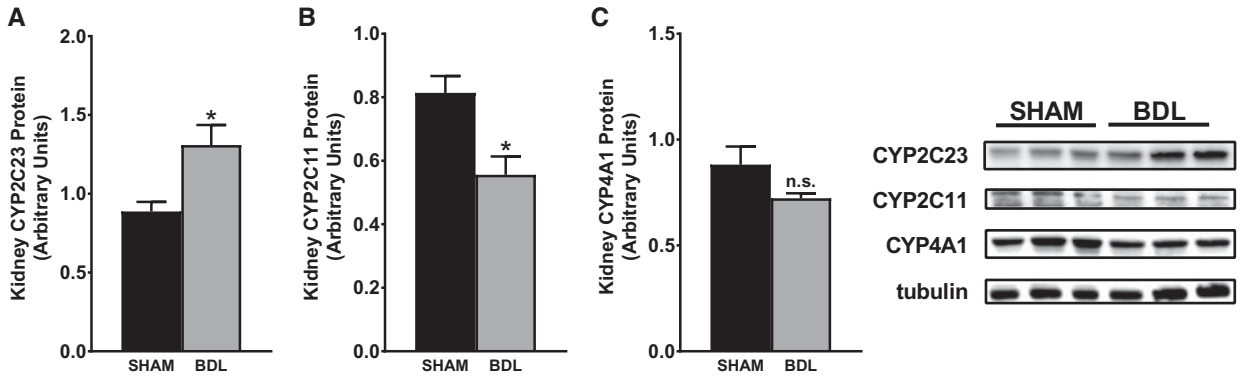

FIGURE 5: CYP isoform protein expression in kidney is altered in cirrhotic rats.
Representative western blots of (**A**) CYP2C23, (**B**) CYP2C11 and (**C**) CYP4A1 protein expression in renal cortical tissue from rats at 5 weeks after sham or BDL surgery. Protein expression was determined by densitometric analyses normalized with tubulin. Values are represented as the mean ± SEM; $n = 8$ per group. *$P < 0.05$ versus sham group.

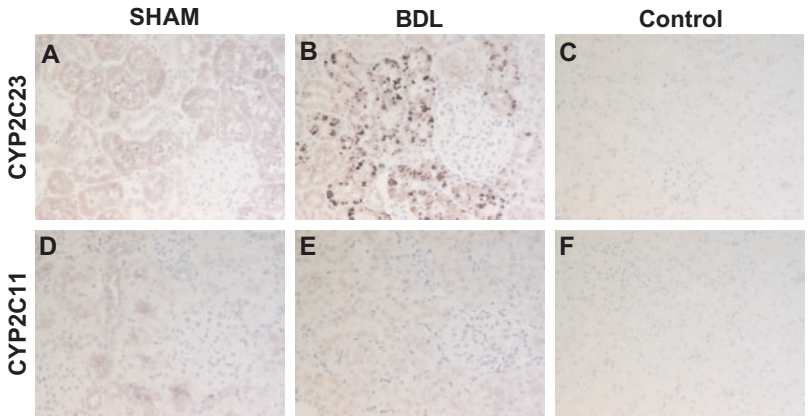

FIGURE 6: Immunolocalization of CYP isoform proteins in kidney.
Immunostaining for CYP2C23 (1:500) (**A**, **B**) and CYP2C11 (1:200) (**D**, **E**) was conducted in kidney sections from 5-week BDL and sham rats. Representative images are shown. CYP2C23 immunostaining was predominantly localized in cortical tubules and was increased in BDL kidney. CYP2C11 was detected in both cortical and medullary tubules and immunostaining was reduced in BDL kidney. No staining was observed when the primary antibody was omitted (**C**, **F**). Immunopositive area appears in purple (ImmPACT VIP Peroxidase Substrate) with blue hematoxylin counterstain. Original magnification, ×200.

detected in both cortical and medullary tubules and immunostaining was reduced at 5 weeks post-BDL compared with sham-operated animals (Figure 6D, E). Together, these data indicate that cirrhosis is associated with alterations in specific CYP enzyme expression at both transcriptional and translational levels in the kidney.

CYP isoform expression in mesenteric vessels during cirrhosis

Splanchnic vasodilatation coupled with intense renal vasoconstriction is the hallmark of the severe hemodynamic alteration seen in advanced liver cirrhosis that is commonly associated with functional renal failure. Given the alterations in CYP expression in the kidney during cirrhosis, we wanted to ascertain if and how CYP expression is regulated in the mesenteric vessels. As shown in Figure 7, CYP2C23 protein expression was reduced by 85% in 5-week BDL rats compared with sham rats. CYP2C11 expression was increased 2-fold in cirrhotic rats and CYP4A1 expression was increased about 4.5-fold in cirrhotic rats compared with sham rats. qPCR showed gene expression results that trended similarly to the western blot data (data not shown).

Inhibition of CYP epoxygenase expression exacerbates renal dysfunction in cirrhosis

To investigate the pathophysiologic role of the observed changes in CYP enzyme expression on renal functional parameters during cirrhosis, we first measured the CYP metabolite production profile in the urine of BDL versus sham rats at 5 weeks post-surgery. As shown in Figure 8A, LC-ESI-MS/MS analysis revealed an overall increase in vasodilatory epoxygenase metabolites (EETs and DHETs) in BDL rats compared with sham rats. The levels of 20-HETE were below the detection limit in the urine. This suggests that EETs mediate the effects of CYP enzymes on the kidney during cirrhosis. We next examined the effect of blocking epoxygenase-derived EET production on renal function using MSPPOH, a well-known selective epoxygenase inhibitor. Starting on Day 22 post-BDL surgery, the animals received three daily treatments with MSPPOH or vehicle. As shown in Figure 8B, treatment with MSPPOH

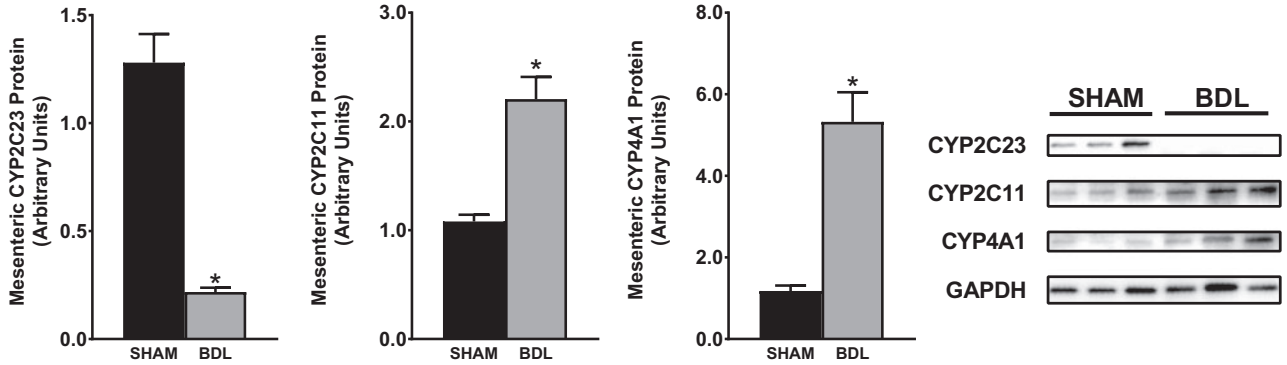

FIGURE 7: CYP isoform protein expression in mesenteric vessels.
Representative western blots of CYP2C23, CYP2C11 and CYP4A1 protein expression in mesenteric vessels from rats at 5 weeks after sham or BDL surgery are shown. Protein expression was determined by densitometric analyses normalized with glyceraldehyde-3-phosphate dehydrogenase (GAPDH). Values are represented as the mean ± SEM; $n = 8$ per group. *$P < 0.05$ versus sham group.

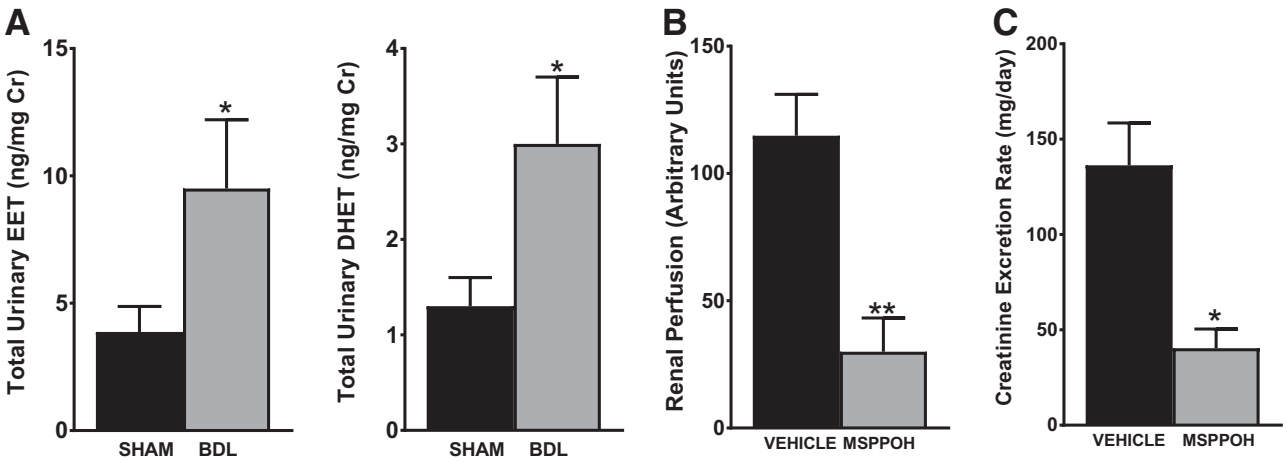

FIGURE 8: Inhibition of CYP epoxygenase exacerbates renal dysfunction in cirrhosis.
(**A**) Urinary levels of CYP eicosanoids were analyzed by LC-ESI-MS. The total EET and DHET levels in sham and BDL animals are shown. Most of the EETs and DHETs were made up of the 14,15- and 11,12-regioisomers. (**B**) Renal perfusion and (**C**) the creatinine excretion rate were measured in BDL rats after treatment with vehicle or MSPPOH. Values are represented as the mean ± SEM; $n = 4–6$ per group.
*$P \leq 0.05$, **$P < 0.01$ versus sham or vehicle group.

resulted in a significant reduction in renal cortical perfusion compared with vehicle treatment. Consistent with the reduced renal perfusion, the creatinine excretion rate was significantly reduced by MSPPOH treatment compared with vehicle treatment (Figure 8C). These results demonstrate that the CYP/EET pathway plays a critical role in modulating renal function during cirrhosis.

DISCUSSION

Renal failure is a major complication of cirrhosis, affecting ~40–80% of patients with end-stage liver disease. The occurrence of renal dysfunction in individuals with cirrhosis portends a poor prognosis. Patients with advanced liver disease and renal failure are at increased risk for death while waiting for liver transplantation and are at a higher risk for complications and reduced survival after transplantation when compared with patients without kidney failure [35, 36]. Renal dysfunction in the setting of liver failure is due mostly to conditions that lead to reduced kidney blood flow (prerenal causes) or from problems within the kidney (intrinsic renal causes). HRS is a unique type of functional kidney failure that complicates advanced chronic liver disease and severe acute fulminant liver failure. HRS is characterized by profound intrarenal vasoconstriction and a marked decline in GFR but without overt histological findings in the kidney.

CYP-derived eicosanoids have many cardiovascular and organ-protective effects. In this study, we investigated the potential role of the CYP/EET pathway in the pathogenesis of renal dysfunction in a rat model of liver cirrhosis. Our key findings were that (i) the BDL model of liver cirrhosis in the rat leads to severe renal dysfunction that is associated with markedly reduced renal cortical perfusion, but without obvious histological changes in the kidney, consistent with HRS; (ii) BDL induced temporal changes in CYP enzyme expression that showed distinct patterns in the kidney versus the mesenteric vessels and (iii) the selective inhibition of CYP epoxygenases in BDL rats resulted in significantly reduced renal function and

renal cortical perfusion. Taken together, our data demonstrate an important role for the CYP/EET pathway in preserving renal function during cirrhosis.

The definitive treatment of HRS is liver transplantation; however, this treatment modality is limited by the shortage of donor organs and the significantly reduced survival of these patients. Once established, HRS may lead to death within a few days. Vasoconstrictor agents like the vasopressin analog terlipressin, with selective activity on splanchnic smooth muscles, have become first-line medical treatment. In places like the USA, where terlipressin is not available, midodrine (an α_1-receptor agonist) is used. Unfortunately, these drugs have limited effects on survival and, for majority of the patients, their use is only aimed as a bridge to liver transplantation [20–22]. Thus, novel treatment options are urgently needed to improve the long-term survival of these patients. The factors that lead to altered renal hemodynamics during cirrhosis are not completely known. The 'splanchnic arterial vasodilation hypothesis' suggests that during advancing cirrhosis, the worsening portal hypertension is associated with increased levels of circulating NO and other vasodilators that lead to splanchnic and peripheral vasodilatation that results in pooling of blood in these vascular beds and therefore a reduction in the effective circulating blood volume and cardiac output [10, 37]. The compensatory and homeostatic mechanisms like the RAAS, the SNS and the non-osmotic release of vasopressin that are activated to reverse this apparent hypovolemia then cause renal vasoconstriction and reduced renal function. Other important contributors to the observed renal vasoconstriction include increased endothelin-1 (ET-1) levels and local reduction in NO production within the kidney despite the elevated circulating levels [33, 38]. Recent reports have also highlighted the important role of inflammation in the development of HRS. Circulating endotoxins and pro-inflammatory cytokines worsen the tenuous hemodynamic state, at least in part by stimulating a further increase in systemic NO levels [9, 39]. Interestingly, the expression of both angiotensin II (Ang-II) and ET-1, key renal vasoconstrictors in this setting, is regulated by the serine protease chymase. Chymase converts Ang-I into Ang-II in an angiotensin-converting enzyme (ACE)-independent way. Indeed, there is evidence that a major fraction of the renal Ang-II concentration is generated via ACE-independent mechanisms. Chymase also converts big ET to ET-1. The expression and activity of chymase are increased in the liver and kidney during cirrhosis and this protease may play a role in the altered hemodynamics of cirrhosis through increased generation of Ang-II and ET-1 within the kidney [40, 41]. Using a rat model of cirrhosis, Sansoe *et al.* [41] showed that inhibition of chymase resulted in improved liver and renal function. Future studies will examine the pathophysiological role of chymases and potentially other proteases in the development of renal dysfunction in cirrhosis. Such studies may benefit from the use of the PROTEASIX tool [42] with a view to identifying novel proteases that mediate the hemodynamic alterations in cirrhosis.

A major aim of this study was to characterize the BDL model as a satisfactory model to study HRS. The BDL model was described many years ago and has become a useful model to study biliary cirrhosis. Over the years, different investigators have described various renal effects of this model [43–45]. Here, by studying renal parameters over time, we have been able to identify key elements that make this model a good one to study HRS. At 5 weeks post-BDL, there was a significant reduction in renal function coupled with a profound reduction in renal cortical perfusion, but without obvious evidence of acute tubular necrosis, features that are consistent with HRS. Our observations corroborate prior findings by Pereira *et al.* [44]. Next, our objective was to use this model to evaluate the expression and functional role of the CYP system in the pathogenesis of renal dysfunction during cirrhosis. In the rat kidney, CYP2C23 and CYP2C11 are the predominant CYP epoxygenases responsible for most of the vasodilatory EET production [46, 47]. Once produced, EETs are metabolized to their less potent DHETs by soluble epoxide hydrolase, which thus regulates EET bioavailability. The sum total of urinary EETs and DHETs is therefore a measure of *in vivo* renal epoxygenase activity. EETs mediate many autocrine and paracrine functions, including the regulation of vascular tone and tubular sodium and water absorption in the kidney. CYP4A1 and other CYP4A isoform enzymes contribute to the formation of 20-HETE. We observed marked changes in CYP isoform expression in the kidney following BDL. There were reciprocal changes in the expression of CYP2C23 and CYP2C11. CYP2C23 expression was significantly increased while CYP2C11 was decreased in the kidney at 5 weeks post-BDL compared with sham-operated rats. The changes were observed in the mRNA expression and also at the level of protein expression as per our western blot and immunohistochemical staining results of the kidney. The reason for the differential expression of these epoxygenases during BDL-induced cirrhosis is not known, but the overall epoxygenase activity was increased in cirrhotic rats as indicated by the significant increase in total EETs and DHETs in the urine (the majority was made up of the 14,15 regioisomer). Our findings suggest an important role for the CYP/EET pathway in maintaining renal function during cirrhosis. This is demonstrated by the worsening of renal function and renal cortical perfusion in BDL rats following treatment with the epoxygenase inhibitor MSPPOH. The effects of other AA metabolites on renal function in cirrhotic rats have been previously reported [48–50]. Systemic and renal production of thromboxane A2, a potent renal vasoconstrictor, is increased during cirrhosis and has been proposed to contribute to renal dysfunction in cirrhosis. However, treatment with a thromboxane synthase inhibitor failed to reverse HRS in affected patients [51]. On the other hand, vasodilator prostaglandins (PGs) like PGE2 are involved in the preservation of renal blood flow during cirrhosis [52]. Using an isolated perfused kidney model from cirrhotic rats, Miyazono *et al.* [31] showed that NO-independent and PG-independent vasodilation remain after inhibition of both PG and NO production that is likely mediated by an EET [31]. Interestingly, Sacerdoti *et al.* [53] found significantly elevated urinary excretion of 20-HETE in patients with cirrhosis and ascites. Based on its known vasoconstrictor effects, the authors concluded that 20-HETE may participate in the renal functional abnormalities associated with cirrhosis. In that study, urinary

EET excretion was not measured. The renal production of EETs, which act as EDHFs, is likely upregulated as a compensatory mechanism to counteract the effects of increased endogenous vasoconstrictors and to reduce the impact of locally decreased NO production in the kidney. In addition to the vascular effects, the increased EETs may also play a role in water and salt handling by the kidneys during cirrhosis. The development of ascites and volume overload in cirrhosis is due at least in part to increased tubular reabsorption of salt and water [54]. In this study, we found a marked increase in the tubular expression of CYP2C23. EETs inhibit sodium reabsorption by the epithelial sodium channel (ENaC) [27], therefore the observed increase in expression of CYP2C23 in the tubular epithelial cells supports a homeostatic role of this pathway during cirrhosis. The net increase in kidney EET levels may be important in limiting sodium reabsorption by the ENaC. Such a protective role is consistent with our data showing that CYP2C23 expression is reduced in the mesenteric vessels, which is the site of expression of many other vasodilators and is a key initiating factor to the hemodynamic derangement seen in cirrhosis. Thus the differential, tissue-specific expression of CYP enzymes likely has important pathophysiological relevance. In contrast to our study findings and also that of Miyazono *et al.* [31], both of which used BDL-induced cirrhosis rat models, Sacerdoti *et al.* [55], studying a carbon tetrachloride–induced cirrhosis model, reported a decrease in renal EETs in cirrhotic rats, which was specifically linked to a decrease in 11,12-EET levels. Apart from the methodologic differences, that study did not measure the levels of 14,15-EET, which has since been found to be the major EET produced in the kidney. In addition to its vasodilator properties, EETs are able to protect tissues through other mechanisms, including anti-inflammatory, antiapoptotic and antioxidative effects. In fact, previous studies by our group and others have demonstrated that EETs mediate organ protection in a number of preclinical models of human diseases, including but not limited to diabetes, hypertension, ischemic cardiac injury and calcineurin-induced hypertension and nephrotoxicity [25, 30, 56, 57]. Our current findings are in total agreement with the above and demonstrate a beneficial effect of the CYP/EET system on renal function in cirrhotic rats. Di Pascoli *et al.* [58] reported an improvement in portal hypertension in rats with carbon tetrachloride–induced cirrhosis following inhibition of EET production by MSPPOH treatment. They concluded that the treatment would result in beneficial effects in patients with cirrhosis and portal hypertension [58]. Our findings indicate that such a treatment will have detrimental effects on kidney function. Also, Herse *et al.* [59], using a rat model of preeclampsia, reported that treatment with MSPPOH resulted in a reduction in EET production and led to improvement in the preeclamptic syndrome. This clearly seems to be contradictory to the many studies showing beneficial roles of the CYP/EET system in the regulation of renal and cardiovascular function. As alluded to by the authors of that report, this suggests that the role of EETs has to be specifically defined for the given pathophysiological condition. While one previous study found changes in CYP expression in the kidneys of BDL rats very much in keeping with our observations [31], our report is the first to directly connect the relevance of altered renal CYP expression to renal function changes in cirrhotic rats. Our study is also the first to show time-dependent changes in renal CYP expression during cirrhosis. Furthermore, we have identified differential expression patterns of CYP in the kidney and mesenteric vessels, which likely has pathophysiological and therapeutic importance. Our data suggest that the observed changes in CYP expression are most likely a homeostatic response to maintain renal perfusion and renal function. In this study, we used MS to measure urine EET and DHET levels. MS is a very sensitive analytical technique that identifies molecules based on their mass:charge ratio. It may be used to analyze both pure samples and complex mixtures and the results are shown as spectra of the relative abundance of detected ions versus the mass:charge ratio. The capability of MS is markedly increased by using it in tandem with separation techniques, including gas and liquid chromatography (GC-MS and LC-MS, respectively). A key drawback of this technique is that there are limited databases available for the mass spectra. Selected reaction monitoring, also known as MRM, is a common and sensitive method used for spectrometric quantitation. This type of quantitation makes use of unique fragmentations for the compounds under analysis, and with an LC method, the chromatographic retention time of the precursor. A limitation of this is that very different molecules can yield the same MRM pairs. This is uncommon however, and most MRM procedures include a 'validating' MRM that ensures that the quantification was derived from the correct compound.

In conclusion, we found the BDL model to be a satisfactory animal model to study HRS. The study demonstrates that the renal CYP/EET pathway is upregulated in experimental cirrhosis induced by BDL. Our observations indicate that the CYP/EET system might represent a novel therapeutic target for modulating renal dysfunction in advanced cirrhosis.

ACKNOWLEDGEMENTS

We thank Dr Michael Thomas and the Medical College of Wisconsin MS Core Laboratory for technical assistance and helpful discussions. We would also like to thank Dr Laurens Holmes (Clinical and Translational Science Institute of Southeast Wisconsin, Medical College of Wisconsin) for statistical assistance.

FUNDING

This study was funded by the Department of Medicine, Medical College of Wisconsin (to M.M.Y.), a Research Starter Grant from PhRMA Foundation USA (to Md. A.H.K.), National Institutes of Health Grant DK103616 and VA Grant BX002256 (to J.D.I.) and grants from the Dr Ralph and Marian Falk Medical Research Trust Bank of America (to J.D.I.). We acknowledge support from the UAB-UCSD O'Brien Core Center for Acute Kidney Injury Research (NIH P30-DK079337) for creatinine measurements in this project.

CONFLICT OF INTEREST STATEMENT

None declared.

REFERENCES

1. Angeli P, Gines P, Wong F. Diagnosis and management of acute kidney injury in patients with cirrhosis: revised consensus recommendations of the International Club of Ascites. *Gut* 2015; 64: 531–537
2. Arroyo V, Gines P, Gerbes AL *et al.* Definition and diagnostic criteria of refractory ascites and hepatorenal syndrome in cirrhosis. International Ascites Club. *Hepatology* 1996; 23: 164–176
3. Fernandez J, Acevedo J, Prado V *et al.* Clinical course and short-term mortality of cirrhotic patients with infections other than spontaneous bacterial peritonitis. *Liver Int* 2017; 37: 385–395
4. Ginès P, Guevara M, Arroyo V *et al.* Hepatorenal syndrome. *Lancet* 2003; 362: 1819–1827
5. Gines P, Schrier RW. Renal failure in cirrhosis. *N Engl J Med* 2009; 361: 1279–1290
6. Weil D, Levesque E, McPhail M *et al.* Prognosis of cirrhotic patients admitted to intensive care unit: a meta-analysis. *Ann Intensive Care* 2017; 7: 33
7. Guevara M, Gines P. Hepatorenal syndrome. *Dig Dis* 2005; 23: 47–55
8. Ruiz-del-Arbol L, Monescillo A, Arocena C *et al.* Circulatory function and hepatorenal syndrome in cirrhosis. *Hepatology* 2005; 42: 439–447
9. Guarner C, Soriano G, Tomas A *et al.* Increased serum nitrite and nitrate levels in patients with cirrhosis: relationship to endotoxemia. *Hepatology* 1993; 18: 1139–1143
10. Martin PY, Gines P, Schrier RW. Nitric oxide as a mediator of hemodynamic abnormalities and sodium and water retention in cirrhosis. *N Engl J Med* 1998; 339: 533–541
11. Ruiz-del-Arbol L, Urman J, Fernandez J *et al.* Systemic, renal, and hepatic hemodynamic derangement in cirrhotic patients with spontaneous bacterial peritonitis. *Hepatology* 2003; 38: 1210–1218
12. Sole C, Sola E, Morales-Ruiz M *et al.* Characterization of inflammatory response in acute-on-chronic liver failure and relationship with prognosis. *Sci Rep* 2016; 6: 32341
13. Wiest R, Das S, Cadelina G *et al.* Bacterial translocation in cirrhotic rats stimulates eNOS-derived NO production and impairs mesenteric vascular contractility. *J Clin Invest* 1999; 104: 1223–1233
14. Alqahtani SA, Fouad TR, Lee SS. Cirrhotic cardiomyopathy. *Semin Liver Dis* 2008; 28: 59–69
15. Krag A, Bendtsen F, Henriksen JH *et al.* Low cardiac output predicts development of hepatorenal syndrome and survival in patients with cirrhosis and ascites. *Gut* 2010; 59: 105–110
16. Bichet D, Szatalowicz V, Chaimovitz C *et al.* Role of vasopressin in abnormal water excretion in cirrhotic patients. *Ann Intern Med* 1982; 96: 413–417
17. Epstein M, Weitzman RE, Preston S *et al.* Relationship between plasma arginine vasopressin and renal water handling in decompensated cirrhosis. *Miner Electrolyte Metab* 1984; 10: 155–165
18. Henriksen JH, Ring-Larsen H. Hepatorenal disorders: role of the sympathetic nervous system. *Semin Liver Dis* 1994; 14: 35–43
19. Schneider AW, Kalk JF, Klein CP. Effect of losartan, an angiotensin II receptor antagonist, on portal pressure in cirrhosis. *Hepatology* 1999; 29: 334–339
20. Boyer TD, Sanyal AJ, Wong F *et al.* Terlipressin plus albumin is more effective than albumin alone in improving renal function in patients with cirrhosis and hepatorenal syndrome type 1. *Gastroenterology* 2016; 150: 1579–1589.e2
21. Sanyal AJ, Boyer T, Garcia-Tsao G *et al.* A randomized, prospective, double-blind, placebo-controlled trial of terlipressin for type 1 hepatorenal syndrome. *Gastroenterology* 2008; 134: 1360–1368
22. Wong F, Pappas SC, Boyer TD *et al.* Terlipressin improves renal function and reverses hepatorenal syndrome in patients with systemic inflammatory response syndrome. *Clin Gastroenterol Hepatol* 2017; 15: 266–272
23. Brash AR. Arachidonic acid as a bioactive molecule. *J Clin Invest* 2001; 107: 1339–1345
24. Imig JD. Eicosanoid regulation of the renal vasculature. *Am J Physiol Renal Physiol* 2000; 279: F965–F981
25. Imig JD, Zhao X, Capdevila JH *et al.* Soluble epoxide hydrolase inhibition lowers arterial blood pressure in angiotensin II hypertension. *Hypertension* 2002; 39: 690–694
26. McGiff JC, Quilley J. 20-HETE and the kidney: resolution of old problems and new beginnings. *Am J Physiol* 1999; 277: R607–R623
27. Pavlov TS, Ilatovskaya DV, Levchenko V *et al.* Effects of cytochrome P-450 metabolites of arachidonic acid on the epithelial sodium channel (ENaC). *Am J Physiol Renal Physiol* 2011; 301: F672–F681
28. Roman RJ. P-450 metabolites of arachidonic acid in the control of cardiovascular function. *Physiol Rev* 2002; 82: 131–185
29. Sato Y, Sato W, Maruyama S *et al.* Midkine regulates BP through cytochrome P450-derived eicosanoids. *J Am Soc Nephrol* 2015; 26: 1806–1815
30. Yeboah MM, Hye Khan MA, Chesnik MA *et al.* The epoxyeicosatrienoic acid analog PVPA ameliorates cyclosporine-induced hypertension and renal injury in rats. *Am J Physiol Renal Physiol* 2016; 311: F576–F585
31. Miyazono M, Zhu D, Nemenoff R *et al.* Increased epoxyeicosatrienoic acid formation in the rat kidney during liver cirrhosis. *J Am Soc Nephrol* 2003; 14: 1766–1775
32. Martinez-Prieto C, Ortiz MC, Fortepiani LA *et al.* Haemodynamic and renal evolution of the bile duct-ligated rat. *Clin Sci* 2000; 98: 611–617
33. Miyazono M, Garat C, Morris KG Jr et al. Decreased renal heme oxygenase-1 expression contributes to decreased renal function during cirrhosis. *Am J Physiol Renal Physiol* 2002; 283: F1123–F1131
34. Zhou Y, Chang HH, Du J *et al.* Renal epoxyeicosatrienoic acid synthesis during pregnancy. *Am J Physiol Renal Physiol* 2005; 288: F221–F226
35. Gonwa TA, Klintmalm GB, Levy M *et al.* Impact of pretransplant renal function on survival after liver transplantation. *Transplantation* 1995; 59: 361–365
36. Nair S, Verma S, Thuluvath PJ. Pretransplant renal function predicts survival in patients undergoing orthotopic liver transplantation. *Hepatology* 2002; 35: 1179–1185
37. Schrier RW, Arroyo V, Bernardi M *et al.* Peripheral arterial vasodilation hypothesis: a proposal for the initiation of renal sodium and water retention in cirrhosis. *Hepatology* 1988; 8: 1151–1157
38. Kapoor D, Redhead DN, Hayes PC *et al.* Systemic and regional changes in plasma endothelin following transient increase in portal pressure. *Liver Transpl* 2003; 9: 32–39
39. Claria J, Stauber RE, Coenraad MJ *et al.* Systemic inflammation in decompensated cirrhosis: characterization and role in acute-on-chronic liver failure. *Hepatology* 2016; 64: 1249–1264
40. Park S, Bivona BJ, Ford SM Jr *et al.* Direct evidence for intrarenal chymase-dependent angiotensin II formation on the diabetic renal microvasculature. *Hypertension* 2013; 61: 465–471
41. Sansoe G, Aragno M, Mastrocola R *et al.* Role of chymase in the development of liver cirrhosis and its complications: experimental and human data. *PLoS One* 2016; 11: e0162644
42. Klein J, Eales J, Zurbig P *et al.* Proteasix: a tool for automated and large-scale prediction of proteases involved in naturally occurring peptide generation. *Proteomics* 2013; 13: 1077–1082
43. Kountouras J, Billing BH, Scheuer PJ. Prolonged bile duct obstruction: a new experimental model for cirrhosis in the rat. *Br J Exp Pathol* 1984; 65: 305–311
44. Pereira RM, dos Santos RA, Oliveira EA *et al.* Development of hepatorenal syndrome in bile duct ligated rats. *World J Gastroenterol* 2008; 14: 4505–4511
45. Poo JL, Estanes A, Pedraza-Chaverri J *et al.* Chronology of portal hypertension, decreased sodium excretion, and activation of the renin–angiotensin system in experimental biliary cirrhosis. *Rev Invest Clin* 1997; 49: 15–23
46. Holla VR, Makita K, Zaphiropoulos PG *et al.* The kidney cytochrome P-450 2C23 arachidonic acid epoxygenase is upregulated during dietary salt loading. *J Clin Invest* 1999; 104: 751–760
47. Zhao X, Pollock DM, Inscho EW *et al.* Decreased renal cytochrome P450 2C enzymes and impaired vasodilation are associated with angiotensin salt-sensitive hypertension. *Hypertension* 2003; 41: 709–714
48. Dagher L, Moore K. The hepatorenal syndrome. *Gut* 2001; 49: 729–737
49. Zipser RD, Radvan GH, Kronborg IJ *et al.* Urinary thromboxane B2 and prostaglandin E2 in the hepatorenal syndrome: evidence for increased vasoconstrictor and decreased vasodilator factors. *Gastroenterology* 1983; 84: 697–703
50. Laffi G, La Villa G, Pinzani M *et al.* Arachidonic acid derivatives and renal function in liver cirrhosis. *Semin Nephrol* 1997; 17: 530–548
51. Zipser RD, Kronborg I, Rector W *et al.* Therapeutic trial of thromboxane synthesis inhibition in the hepatorenal syndrome. *Gastroenterology* 1984; 87: 1228–1232
52. Sacerdoti D, Merlo A, Merkel C *et al.* Redistribution of renal blood flow in patients with liver cirrhosis. The role of renal PGE2. *J Hepatol* 1986; 2: 253–261

53. Sacerdoti D, Balazy M, Angeli P *et al.* Eicosanoid excretion in hepatic cirrhosis. Predominance of 20-HETE. *J Clin Invest* 1997; 100: 1264–1270
54. Kim SW. Dysregulation of ENaC in animal models of nephrotic syndrome and liver cirrhosis. *Electrolyte Blood Press* 2006; 4: 23–34
55. Sacerdoti D, Escalante BA, Schwartzman ML *et al.* Renal cytochrome P-450-dependent metabolism of arachidonic acid in cirrhotic rats. *J Hepatol* 1991; 12: 230–235
56. Elmarakby AA, Faulkner J, Al-Shabrawey M *et al.* Deletion of soluble epoxide hydrolase gene improves renal endothelial function and reduces renal inflammation and injury in streptozotocin-induced type 1 diabetes. *Am J Physiol Regul Integr Comp Physiol* 2011; 301: R1307–R1317
57. Khan MA, Liu J, Kumar G *et al.* Novel orally active epoxyeicosatrienoic acid (EET) analogs attenuate cisplatin nephrotoxicity. *FASEB J* 2013; 27: 2946–2956
58. Di Pascoli M, Zampieri F, Verardo A *et al.* Inhibition of epoxyeicosatrienoic acid production in rats with cirrhosis has beneficial effects on portal hypertension by reducing splanchnic vasodilation. *Hepatology* 2016; 64: 923–930
59. Herse F, Lamarca B, Hubel CA *et al.* Cytochrome P450 subfamily 2J polypeptide 2 expression and circulating epoxyeicosatrienoic metabolites in preeclampsia. *Circulation* 2012; 126: 2990–2999

Received: 14.6.2017; Editorial decision: 24.11.2017

Nephrol Dial Transplant (2018) 33: 1343–1353
doi: 10.1093/ndt/gfx349
Advance Access publication 5 February 2018

ORIGINAL ARTICLE

Glutamine metabolism via glutaminase 1 in autosomal-dominant polycystic kidney disease

Irfana Soomro[1,2,3], Ying Sun[1,2], Zhai Li[1,2,3], Lonnette Diggs[4], Georgia Hatzivassiliou[5], Ajit G. Thomas[6], Rana Rais[6,7], Barbara S. Slusher[6,7], Stefan Somlo[4] and Edward Y. Skolnik[1,2,8,9]

[1]Division of Nephrology, New York University Langone Medical Center, New York, NY, USA, [2]The Helen L. and Martin S. Kimmel Center for Biology and Medicine, New York University Langone Medical Center, New York, NY, USA, [3]Skirball Institute for Biomolecular Medicine, New York University Langone Medical Center, New York, NY, USA, [4]Department of Medicine, Yale University School of Medicine, New Haven, CT, USA, [5]Cancer Immunology, Genentech, South San Francisco, CA, USA, [6]Department of Drug Discovery, Johns Hopkins University School of Medicine, Baltimore, MD, USA, [7]Department of Neurology, Johns Hopkins University School of Medicine, Baltimore, MD, USA, [8]Department of Biochemistry, New York University Langone Medical Center, New York, NY, USA and [9]Department of Molecular Pharmacology and Molecular Pathogenesis, New York University Langone Medical Center, New York, NY, USA

Correspondence and offprint requests to: Irfana Soomro; E-mail: Irfana.Soomro@nyumc.org; Edward Y. Skolnik; E-mail: Edward.Skolnik@nyumc.org; Twitter handle: @SoomroIrfana

ABSTRACT

Background. Metabolism of glutamine by glutaminase 1 (GLS1) plays a key role in tumor cell proliferation via the generation of ATP and intermediates required for macromolecular synthesis. We hypothesized that glutamine metabolism also plays a role in proliferation of autosomal-dominant polycystic kidney disease (ADPKD) cells and that inhibiting GLS1 could slow cyst growth in animal models of ADPKD.

Methods. Primary normal human kidney and ADPKD human cyst-lining epithelial cells were cultured in the presence or absence of two pharmacologic inhibitors of GLS1, bis-2-(5-phenylacetamido-1,2,4-thiadiazol-2-yl)ethyl sulfide 3 (BPTES) and CB-839, and the effect on proliferation, cyst growth in collagen and activation of downstream signaling pathways were assessed. We then determined if inhibiting GLS1 *in vivo* with CB-839 in the *Aqp2-Cre; Pkd1*$^{fl/fl}$ and *Pkhd1-Cre; Pkd1*$^{fl/fl}$ mouse models of ADPKD slowed cyst growth.

Results. We found that an isoform of GLS1 (GLS1-GAC) is upregulated in cyst-lining epithelia in human ADPKD kidneys and in mouse models of ADPKD. Both BPTES and CB-839 blocked forskolin-induced cyst formation *in vitro*. Inhibiting GLS1 *in vivo* with CB-839 led to variable outcomes in two mouse models of ADPKD. CB-839 slowed cyst growth in *Aqp2-Cre; Pkd1*$^{fl/fl}$ mice, but not in *Pkhd1-Cre; Pkd1*$^{fl/fl}$ mice. While CB-839 inhibited mammalian target of rapamycin (mTOR) and MEK activation in *Aqp2-Cre; Pkd1*$^{fl/fl}$, it did not in *Pkhd1-Cre; Pkd1*$^{fl/fl}$ mice.

Conclusion. These findings provide support that alteration in glutamine metabolism may play a role in cyst growth. However, testing in other models of PKD and identification of the compensatory metabolic changes that bypass GLS1 inhibition will be critical to validate GLS1 as a drug target either alone or when combined with inhibitors of other metabolic pathways.

Keywords: ADPKD, glutaminase 1, glutamine, metabolism, Warburg effect for ESRD

INTRODUCTION

Autosomal-dominant polycystic kidney disease (ADPKD) affects more than 12 million people worldwide and is a common cause of end-stage kidney disease. In the majority of cases,